Ankara University
Institute of Nuclear Sciences

Journal of Nuclear Sciences

Determination of the Mass Attenuation Coefficient, Effective Atomic Number and Electron Density for Manganese Nano Hydroxyapatite by using 778-1457 keV Gamma Rays

O. K. Koksal[1]*, E. Cengiz[2], G. Apaydın[1], A. Tozar[3], İ. H. Karahan[3]

ORCID: 0000-0003-2671-6683, -----

[1]Department of Physics, Faculty of Sciences, Karadeniz Technical University, 61800, Trabzon, Turkey

[2]Department of Fundamental Sciences, Faculty of Engineering, Alanya Alaaddin Keykubat University, 07450, Antalya, Turkey

[3]Department of Physics, Faculty of Science and Literature, Mustafa Kemal University, Hatay,Turkey

ABSTRACT

In this study, manganese nano substituted hydroxyapatite artificial bone powders (nMnHAp) have been investigated experimentally by means of mass attenuation coefficients, effective atomic numbers and electron densities. The samples were irradiated using 778 keV, 964 keV, 1085 keV, 1112 keV, 1408 keV and 1457 keV gamma photons from [152]Eu source .The gamma photons from the source were counted by using a HPGe gamma-ray spectroscopy. The mass attenuation coefficients of the hydroxyapatites artificial bone powders (including hydroxyapatite without any substituted metal and real bone powder) were compared with each other. This study has been dealt with as a guide to medical field. Also the results have been evaluated in terms of the electron density and effective atomic number.

Keywords: Mass attenuation coefficient, Manganese substituted hydroxyapatite, Gamma rays, Europium-152, Transmission method

1. Introduction

The mass attenuation coefficient is a measure of the average number of interactions between transmitted photons from the sample. They depend on photon energy of the source and the atomic number of an element. Only atomic number is not responsible for photon interactions between photon and hydroxyapatite at the interested energy. The reason for this condition is also associated with the electron density and effective atomic number of an element. The partial cross sections are relative to interaction on the different elemental number. This number is named the effective atomic number for the manganese substituted hydroxyapatite [1].

Hydroxyapatite (HAp) is a synthetic compound naturally found in human tooth mines and bones [2]. HAp is utilized in different practises like fluorescent lamps [3], material for fuel cell [4], or an adsorption and stabilization matrix for radioactive waste and harmful metals [5]. Besides, HAp is used as bone filling material due to its biocompatibility [6, 7], scaffold [8] and metal coating material [9-11]. HAp is biocompatible and bioactive but since of its poor mechanical properties it makes its use difficult as an implant material. Therefore, more robust metal is added to hydroxyapatite, to increase the strength of the sample without compromising the biocompatibility.

---

*Corresponding author.

When looking previous studies, there are available HA-based bio composites such as HA alumina, HA-zirconia, HA-biocam and HAw (viscous) composites [12].

In this study, manganese was added to synthetic bone at different concentrations. There are several reasons for adding manganese to hydroxyapatite. When manganese is added to the structure of hydroxyapatite, it increases their density without converting the HAp phase. It also has a positive effect on the binding to the bone [13].

Many investigators [14-18] have focussed on the phenomena of mass attenuation of different material. But there is not any gamma ray attenuation coefficient value experimentally for the metal substituted hydroxyapatite samples. It is important to know how much gamma radiation will be absorbed when used in bone treatments. Because after the bone is treated, it is important to reveal how much radiation will be kept in the body as a result of gamma rays. It is well known that the energies of ^{153}Sm (γ 103 keV, β 640keV, β 710 keVand β 810 keV) are used for the treatment of metastatic bone cancers.

The main purpose of this publication is to reveal the gamma-ray attenuation coefficient of the manganese substituted hydroxyapatite when the samples are exposed to the gamma ray radiation. This study aims to evaluate gamma ray attenuation coefficients in terms of electron density and effective atomic number.

2. Experimental Procedure and Theoretical Background

Firstly, the measurement was carried out without any sample. Then the transmitted photons were counted from hydroxyapatite, real bone powder and manganese substituted hydroxyapatite. The gamma-ray attenuation coefficients were calculated with using well known Lambert Beer equation for hydroxyapatite, real bone powder and manganese substituted Nano hydroxyapatite samples

$$I = I_0 e^{-\mu x} = I_0 e^{-\left(\frac{\mu}{\rho}\right)d} \qquad (1)$$

where I_0 is incident beam to the detector from the gamma-ray source without any absorber. I is transmitted beam from the sample to the detector. d is the mass per unit area (g/cm^2) and μ/ρ is the mass attenuation coefficient(cm^2/g).

The mass attenuation coefficient $(\mu/\rho)_c$ is determined by using the mixture rule for present samples.

$$(\mu/\rho)_c = \sum_i W_i (\mu/\rho)_i \qquad (2)$$

where W_i and $(\mu/\rho)_i$ are the weight fraction and mass attenuation coefficient of the ith constituent element, respectively. For a chemical compound, the fraction by weight is given by Eq.(3).

$$W_i = \frac{n_i A_i}{\sum_i n_i A_i} \qquad (3)$$

where A_i is the atomic weight of the i*th* element and n_i is the number of formula units.

Theoretical values of the gamma ray attenuation coefficients are taken from XCOM data base [19]. The values of the gamma ray attenuation coefficients were used to calculate the molecular cross-section ($\sigma_{t,m}$) by the following formula:

$$\sigma_{t,m} = \frac{1}{N} \left(\frac{\mu}{\rho}\right)_c \sum_i (n_i A_i) \qquad (4)$$

where N is the Avogadro number. The other terms were defined before.Total atomic cross-section ($\sigma_{t,a}$) can be defined using the formula (4) as

$$\sigma_{t,a} = \frac{\sigma_{t,m}}{\sum_i n_i} = \frac{1}{N} \sum_i (f_i A_i) \left(\frac{\mu}{\rho}\right)_i \qquad (5)$$

where $f_i = n_i / \sum_i n_i$ is the fractional abundance of element i with regard to number of atoms. The total electronic cross section $\sigma_{t,el}$ for the individual elements is expressed by the equation below

$$\sigma_{t,el} = \frac{1}{N} \sum_i \frac{f_i A_i}{Z_i} \left(\frac{\mu}{\rho}\right)_i \qquad (6)$$

where Z_i is the atomic number of the i*th* element in a molecule. The total atomic and electronic cross-sections are related to the effective atomic number (Z_{eff}) as below [14]

$$Z_{eff} = \frac{\sigma_{t,a}}{\sigma_{t,el}} \qquad (7)$$

The electron density N_{el} can be derived by using expressions (2) and (6)

$$N_{el} = \frac{(\mu/\rho)_c}{\sigma_{el}} = \frac{N}{M} Z_{eff} \sum_i n_i \qquad (8)$$

The effective atomic numbers and electron densities for the nMnHAp samples were calculated using equations (7) and (8), respectively with the energies shown in Table 1.

In order to determine gamma-ray attenuation coefficients, the samples were prepared at a 10 MPa pressure through a hydraulic press for a few minutes to get a pellet form. The specimens have diameter as 13 mm and almost same thicknesses.

The schematic arrangement (Fig. 1) of the experimental set-up was prepared for the primary incident source (^{152}Eu), the sample (S) and the detector system (D) as shown in Fig. 1, where the primary beam hits the sample. High purity germanium (HPGe) detector was used to count the transmitted gamma photons. The detector is
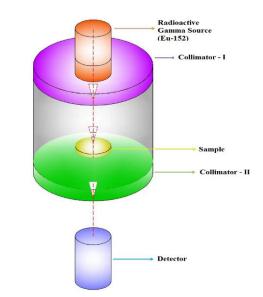
fabricated by Ortec HPGe. It has relative efficiency of %25 at 1.33 MeV and an energy resolution of 1.85 keV at 1.33 MeV. The gamma-ray energies from [152]Eu source given in Table 1 was used in this work[20].

3. Results and discussion

The theoretical gamma-ray attenuation coefficients were computed using the XCOM software [21] for the samples except real bone powder are tabulated at the Table 1.

It is seen in Table 1 and 2, that experimental values are in good agreement with theoretical values. Since no value can be found in the literature regarding the gamma-ray attenuation coefficient for any nHAp samples, no comparison can be made with a value in the previous studies. In this sense, this study has also a reference feature.

The variation between electron density and effective atomic number is shown in Fig. 2.

Fig. 1 *A schematic diagram of experimental arrangement*

Table 1. The theoretical gamma-ray attenuation coefficient μ/ρ (cm^2/g) for nMnHAp, nHAp and real bone.

Samples	μ/ρ 778.90 keV	μ/ρ 964.07keV	μ/ρ 1085.83 keV	μ/ρ 1112.07keV	μ/ρ 1408.01 keV	μ/ρ 1457.64keV
Real Bone	---	---	---	---	---	---
HAp	0.0712	0.0649	0.0612	0.0604	0.0536	0.0527
MnHAp0.5	0.0687	0.0620	0.0581	0.0574	0.0510	0.0501
MnHAp1.0	0.0710	0.0641	0.0604	0.0597	0.0530	0.0520
MnHAp1.5	0.0678	0.0611	0.0576	0.0568	0.0504	0.0495

* Mass attenuation coefficients **μ/ρ** calculated from XCOM NIST

Table 2. The experimental gamma-ray attenuation coefficient μ/ρ (cm^2/g) for nMnHAp, nHAp and real bone.

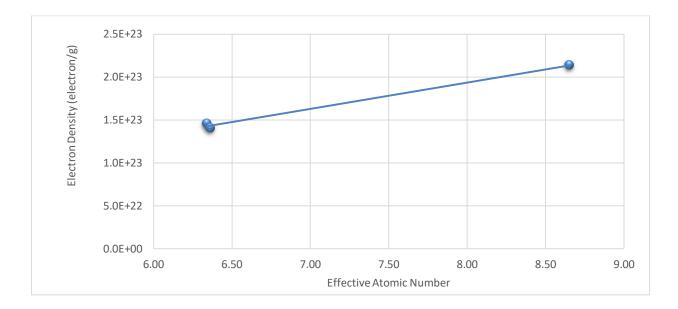| Samples	μ/ρ 778.90 keV	μ/ρ 964.07keV	μ/ρ 1085.83keV	μ/ρ 1112.07 keV	μ/ρ 1408.01 keV	μ/ρ 1457.64keV
Real Bone	0.0831	0.0649	0.0624	0.0601	0.0563	0.0812
HAp	0.0595	0.0666	0.0666	0.0612	0.0536	0.0744
MnHAp 0.5	0.0663	0.0622	0.0525	0.0658	0.0533	0.0463
MnHAp 1.0	0.0745	0.0666	0.0775	0.0667	0.0597	0.0538
MnHAp 1.5	0.0677	0.0577	0.0681	0.0535	0.0603	0.0595

Fig.2 *Effective atomic number versus electron density*

The empirical electron density and effective atomic number of manganese substituted HAp, pure HAp and are presented at the Table 3.

When considering the Fig. 2 and Table 3, it appears that the electron density and the effective atomic number increase in direct proportion with each other. The effective atomic number and the mass attenuation coefficient are directly proportional to each other. This information can be inferred from the Figs. 2 and Table 3. The variation of the coefficients versus effective atomic number and energy values are illustrated in Fig. 3.

Table 2. Effective Atomic Numbers (Z_{eff}) and effective electron density ($N_{el.}$ in units of 10^{+23} electrons g^{-1}) of the samples at 59.5 keV

Samples	$N_{el.}$	Z_{eff}
nMnHAp0.5	1.45	6.34
nMnHAp1.0	2.13	8.65
nMnHAp1.5	1.40	6.36

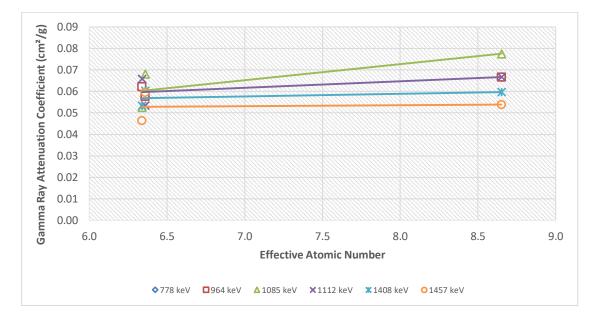***Fig. 3*** *Effective atomic number versus gamma ray attenuation coefficient*

As seen in Fig. 3, the attenuation coefficient of the present samples are proportional to effective atomic numbers. It has been found that the changes in the attenuation coefficients do not seem to be linear to the added manganese. The fluctuations in the attenuation coefficients are observed when the metal is added. It is well known that all of the metal-doped hydroxyapatite samples are metal-exchanged. Briefly, when a metal is added to a hydroxyapatite sample, the metal enters the structure and the some calcium atoms leave from the structure [7, 22, 23]. It is thought that the electron density and effective atomic number can alter when the metal is added to nHA. Therefore, the electron density values and effective atomic number are calculated experimentally. The gamma ray attenuation coefficients versus gamma energies were plotted in Fig. 4.

When the gamma excitation energy increases, the absorption coefficient of MnHAp decreases somehow more than that of real bone. As the excitation energy increases, the interaction with the atoms in the sample decreases and absorbs less radiation. However, it is concluded that the gamma-ray attenuation coefficients of the nMnHAp are very close to real bone and pure hydroxyapatite; respectively when we selected the gamma energy range of approximate 779 to 1457 keV. In future, the gamma-ray attenuation coefficients of the nMnHAp might be determined for the low energy range of below 779 keV.
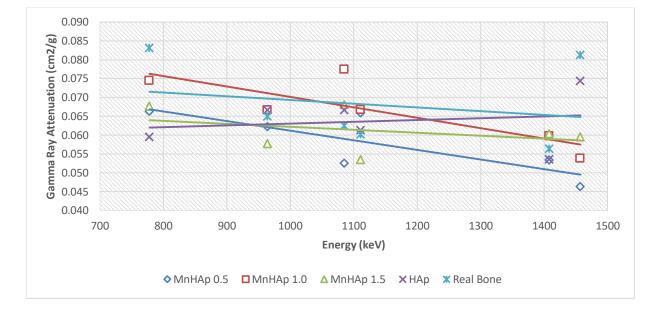

Fig. 4 *The gamma ray attenuation coefficients versus gamma energies for different samples*

Conflict of Interest

The authors have no conflict of interest.

References

[1] S.G. Prasad, K. Parthasaradhi, W.D. Bloomer, Effective atomic numbers for photoabsorption in alloys in the energy region of absorption edges, Radiat Phys Chem, 53, 449-453 (1998).

[2] D.K. Dubey, V. Tomar, Understanding the influence of structural hierarchy and its coupling with chemical environment on the strength of idealized tropocollagen-hydroxyapatite biomaterials, J Mech Phys Solids, 57, 1702-1717 (2009).

[3] D.E. Wagner, K.M. Eisenmann, A.L. Nestor-Kalinoski, S.B. Bhaduri, A microwave-assisted solution combustion synthesis to produce europium-doped calcium phosphate nanowhiskers for bioimaging applications, Acta Biomater, 9, 8422-8432 (2013).

[4] X. Wei, M.Z. Yates, Yttrium-Doped Hydroxyapatite Membranes with High Proton Conductivity, Chem Mater, 24,1738-1743 (2012).

[5] Y. Watanabe, T. Ikoma, Y. Suetsugu, H. Yamada, K. Tamura, Y. Komatsu, J. Tanaka, Y. Moriyoshi, The densification of zeolite/apatite composites using a pulse electric current sintering method: A long-term assurance material for the disposal of radioactive waste, J Eur Ceram Soc, 26, 481-486 (2006).

[6] J. Vamze, M. Pilmane, A. Skagers, Biocompatibility of pure and mixed hydroxyapatite and alpha-tricalcium phosphate implanted in rabbit bone, J Mater Sci-Mater M, 26 (2015).

[7] C.T. Wong, W.W. Lu, W.K. Chan, K.M.C. Cheung, K.D.K. Lukl, D.S. Lu, A.B.M. Rabie, L.F. Deng, J.C.Y. Leong, In vivo cancellous bone remodeling on a strontium-containing hydroxyapatite (Sr-HA) bioactive cement, J Biomed Mater Res A, 68a, 513-521 (2004).

[8] L. Nie, D. Chen, J. Fu, S.H. Yang, R.X. Hou, J.P. Suo, Macroporous biphasic calcium phosphate scaffolds reinforced by poly-L-lactic acid/hydroxyapatite nanocomposite coatings for bone regeneration, Biochem Eng J, 98, 29-37 (2015).

[9] H. Akazawa, Y. Ueno, Low-temperature crystallization and high-temperature instability of hydroxyapatite thin films deposited on Ru, Ti, and Pt metal substrates, Surf Coat Tech, 266, 42-48 (2015).

[10] D. Duraccio, F. Mussano, M.G. Faga, Biomaterials for dental implants: current and future trends, J Mater Sci, 50, 4779-4812 (2015).

[11] M. Razavi, M. Fathi, O. Savabi, D. Vashaee, L. Tayebi, In Vitro Analysis of Electrophoretic Deposited Fluoridated Hydroxyapatite Coating on Micro-arc Oxidized AZ91 Magnesium Alloy for Biomaterials Applications, Metall Mater Trans A, 46a, 1394-1404 (2015).

[12] N. Demirkol, Koyun Hidroksiapatit Esaslı Kompozitlerin Üretimi ve Karakterizasyonu, Fen Bilimleri Enstitüsü, 2013.

[13] H.M. Pandya, P. Anitha, Influence of Manganese on the Synthesis of Nano Hydroxyapatite by Wet Chemical Method for in vitro Applications, International Journal of Medical Research and Review, 3, 394-402 (2015).

[14] K. Singh, H. Singh, V. Sharma, R. Nathuram, A. Khanna, R. Kumar, S.S. Bhatti, H.S. Sahota, Gamma-ray attenuation coefficients in bismuth borate glasses, Nuclear Instruments and Methods in Physics Research Section B: Beam Interactions with Materials and Atoms, 194, 1-6 (2002).

[15] H. Singh, K. Singh, L. Gerward, K. Singh, H.S. Sahota, R. Nathuram, ZnO–PbO–B2O3 glasses as gamma-ray shielding materials, Nuclear Instruments and Methods in Physics Research Section B: Beam

Interactions with Materials and Atoms, 207, 257-262 (2003).

[16] P. Limkitjaroenporn, J. Kaewkhao, P. Limsuwan, W. Chewpraditkul, Physical, optical, structural and gamma-ray shielding properties of lead sodium borate glasses, J Phys Chem Solids, 72, 245-251 (2011).

[17] C.T. Chantler, C.Q. Tran, Z. Barnea, D. Paterson, D. Cookson, D. Balaic, Measurement of the x-ray mass attenuation coefficient of copper using 8.85–20 keV synchrotron radiation, Physical Review A, 64, 062506 (2001).

[18] G. Apaydın, E. Cengiz, E. Tıraşoğlu, V. Aylıkcı, Ö.F. Bakkaloğlu, Studies on mass attenuation coefficients, effective atomic numbers and electron densities for CoCuAg alloy thin film, Phys Scripta, 79, 055302 (2009).

[19] M.J. Berger, J.H. Hubbell, S.M. Seltzer, J.S. Coursey, D.S. Zucker, XCOM: photon cross section database (version 1.2), 1999.

[20] N. Kaya, E. Tıraşoğlu, G. Apaydın, V. Aylıkcı, E. Cengiz, K-shell absorption jump factors and jump ratios in elements between Tm (Z= 69) and Os (Z= 76) derived from new mass attenuation coefficient measurements, Nuclear Instruments and Methods in Physics Research Section B: Beam Interactions with Materials and Atoms, 262, 16-23 (2007).

[21] M.J. Berger, J. Hubbell, XCOM: Photon cross sections on a personal computer, National Bureau of Standards, Washington, DC (USA). Center for Radiation Research, 1987.

[22] M. Honda, K. Kikushima, Y. Kawanobe, T. Konishi, M. Mizumoto, M. Aizawa, Enhanced early osteogenic differentiation by silicon-substituted hydroxyapatite ceramics fabricated via ultrasonic spray pyrolysis route, J Mater Sci-Mater M, 23, 2923-2932 (2012).

[23] J. Wang, T. Nonami, K. Yubata, Syntheses, structures and photophysical properties of iron containing hydroxyapatite prepared by a modified pseudo-body solution, J Mater Sci-Mater M, 19, 2663-2667 (2008).